

Hydrostatic pressure decreases the proton mobility in the hydrated $\text{BaZr}_{0.9}\text{Y}_{0.1}\text{O}_3$ proton conductor

Qianli Chen,^{1,2} Artur Braun,^{1,a)} Alejandro Ovalle,¹ Cristian-Daniel Savaniu,³ Thomas Graule,^{1,4} and Nikolai Bagdassarov⁵

¹Laboratory for High Performance Ceramics, Swiss Federal Laboratories for Materials Science and Technology, Empa, CH-8600 Dübendorf, Switzerland

²Department of Physics, Swiss Federal Institute of Technology, ETH Zürich, CH-8057 Zürich, Switzerland

³School of Chemistry, University of St. Andrews, St Andrews, Fife, KY16 8DA Scotland, United Kingdom

⁴Technische Universität Bergakademie Freiberg, D-09596 Freiberg, Germany

⁵Institut für Geosciences, J. W. Goethe Universität Frankfurt am Main, D-60323 Frankfurt/Main, Germany

(Received 19 April 2010; accepted 22 June 2010; published online 27 July 2010)

Impedance spectroscopy on the hydrated proton conductor $\text{BaZr}_{0.9}\text{Y}_{0.1}\text{O}_3$ at high temperatures shows that the bulk proton conductivity activation energy E_b scales with the strain parameter ϵ , as achieved by hydrostatic pressures up to 2 GPa, suggesting that large lattices favor proton diffusivity. At high temperature, E_b increases upon pressure by 40%. The grain boundary activation energy E_g is around twice as E_b , indicating higher proton mobility in grain boundaries as a result of pressure induced sintering. An expanded lattice with strain parameter $\epsilon > 1$ should have lower E_b , suggesting that thin films expansive tensile strain could have larger proton conductivity. © 2010 American Institute of Physics. [doi:10.1063/1.3464162]

Proton conducting ceramics have the potential for a wide range of applications, for example, solid electrolytes in electrochemical devices such as fuel cells, electrolyzers, and sensors. Compared to conventional solid electrolytes based on oxygen ion conductivity, materials with pronounced proton conductivity are attractive for lowering the operating temperature. Yttrium substituted barium zirconate, a perovskite with ABO_3 structure, in which oxygen vacancies are created by Y-substitution to the Zr at the B-site, is an attractive candidate material.¹ While the fundamental physical and chemical processes of the proton conductivity are not all well known, the current opinion is that in aqueous atmosphere, the vacancy can be filled by oxygen which dissociates from adsorbed water molecule,² and the introduced protons are bound to the lattice oxygen in the octahedron ZrO_6 .³ While literature has not been unambiguous about models and details,^{4,5} proton diffusion can be considered a combination of free diffusion and trapping and escape events.^{6,7} The first state represents free, delocalized diffusion of the protons jumping from one oxygen to another oxygen, forming OH^- , and a very fast localized motion of the OH^- as a reorientation; the second state represents protons trapped on energetically lowered sites near a dopant ion such as Y^{3+} . The fast localized motion of OH^- ions comes with an activation energy in the order of few millielectron volt at moderate temperature;⁶ whereas at elevated temperature, thermal activation may drive the proton to another oxygen site by overcoming an energy barrier in the range of a few hundred millielectron volt,⁷ and thus constituting charge mobility. Not only for improving device applications, but also from a fundamental point of view it is of high interest to understand the relationship of structure parameters and proton transport properties. The potential relations between proton conduction activation energy (E_a) and structure parameters were pointed out as early as 1988 by Scherban,⁸ who found that

the E_a of Yb-doped SrCeO_3 and BaCeO_3 decreases when their oxygen-oxygen distance increases. Our recent findings applying “chemical pressure”—achieved by different synthesis routes—suggest that E_a for bulk proton transport increases with decreasing lattice spacing.^{9,10} In their work on $\text{Ba}_{6-y}\text{Ca}_y\text{Nb}_2\text{O}_{11}$, Ashok¹¹ *et al.* found that an expansion of the unit cell caused by varying the concentration of the A-site element eases the carrier mobility. Wu *et al.*^{12,13} reported that heavily Y-doped BaCO_3 exhibits significantly lower conductivity than those of lightly doped analogs, suggesting that facilitating proton transport based on B-site doping has limitations. While change in the A-site cation size has a direct effect on the lattice volume and also on the proton conductivity, one cannot generally rule out that the different chemical nature of the chosen substituent may have an additional specific influence. The direct method to prove the aforementioned hypothesis is to apply hydrostatic pressure (p)- and temperature (T)-dependent analytical techniques to monitor the proton transport, as was done previously with impedance spectroscopy.¹⁴ To investigate intuitively the change in the lattice volume of the proton conductor, it is technically more challenging to expand the lattice volume. In this work, $\text{BaZr}_{0.9}\text{Y}_{0.1}\text{O}_{2.95}$ (BZY10) was prepared and the structure determined by x-ray diffraction. After hydration, their electrical conductivities were studied at high pressure and high temperature to have a better understanding of the nature of proton transport in those materials.

Two batches of BZY10 were prepared, correspondingly by solid-state reaction (SS)^{9,10,15,16} and sol-gel (SG) synthesis. SG material was prepared starting from barium acetate (99%), zirconium (IV) 2,4-pentanedionate (99%) and yttrium (III) 2-ethylhexanoate (99.8%); concentrated glacial acetic acid (>99%) being used as chelating agent and solvent. The reactants were dissolved in stoichiometric ratios in acetic acid at 353 K and the resulting clear solution was stirred for another 3 h, followed by slow evaporation of the remaining acetic acid on a hot plate. The resultant dark brown syrup remained precipitate-free, leading to very fine powder by heating to 627 K and then to 1573 K to ensure the formation

^{a)} Author to whom correspondence should be addressed. Electronic mail: artur.braun@alumni.ethz.ch. Tel.: +41 44 823 4850. FAX: +41 44 823 4150.

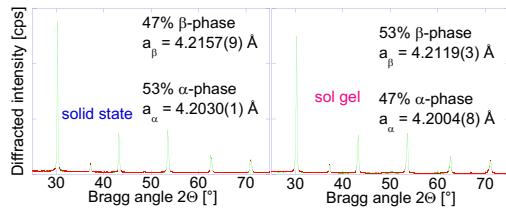


FIG. 1. (Color online) X-ray powder diffractograms of BZY10 prepared by SS and SG route.

of BZY10. Pellets of material were pressed and fired at 1773 K for 12 h for densification, and ground into powder for crystal structure and conductivity measurements.

It has been reported that, depending on synthesis parameters, two isostructural cubic $Pm-3m$ phases may coexist in BZY10: a so-called well conducting β -phase with a larger lattice constant (a), and an α -phase with a smaller lattice constant, as previously revealed using high resolution neutron diffraction data on samples prepared in similar conditions.¹⁷ This is confirmed by the Rietveld refinement of the x-ray diffractograms (see Fig. 1), showing that SS and SG samples are each comprised by two cubic structures with $Pm-3m$ space group, as evidenced by the clear splitting of the peaks: 47% with $a_{SS}=4.2157(9)$ Å and 53% with $a_{SS}=4.2030(1)$ Å for SS, and 53% with $a_{SG}=4.2119(3)$ Å and 47% with $a_{SG}=4.2004(8)$ Å for the SG sample. Line width analysis of the Bragg reflections by the Scherrer equation showed the average crystallite size for SS derived samples was 60–100 nm, and 30–40 nm for the SG derived sample.

The samples were hydrated, also referred to as protonation, like described previously,³ i.e., the samples were heated to an optimized loading temperature of 723 K in H_2O/N_2 flow for 24 h. Electrical impedance spectra were obtained by Solartron 1260 Phase-Gain-Analyzer. A piston-cylinder apparatus was applied on protonated BZY10 powders, 1 GPa $< p < 2$ GPa and 300 K $< T < 680$ K.¹⁸ The analysis of impedance data follows our previous works.^{9,10,15,16}

The temperature and pressure dependence of the conductivities for BZY10 prepared by SS and SG routes are shown respectively in Figs. 2(a) and 2(b). Particularly the low temperatures show that lower pressures provide a higher conductivity than the higher pressures, suggesting that “protons need space” in order to be mobile. This effect seems more pronounced for the low temperatures, where proton jump rotation is known to be the dominant mode,⁶ than for the high temperatures, where the effective jump diffusion sets on.

The E_a for bulk and grain boundary conductivities, shown in Fig. 3, was determined by Arrhenius plot of the

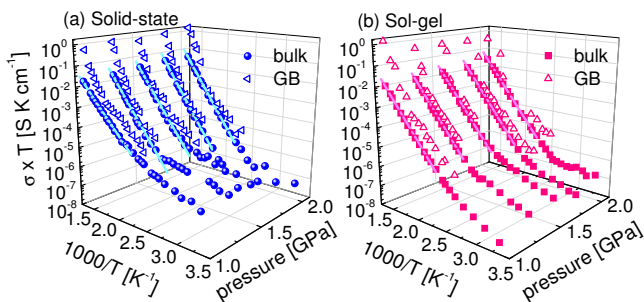


FIG. 2. (Color online) Conductivity of BZY10 at high pressure and high temperature. Bulk and grain boundary conductivity for SS derived samples (a); and for SG derived samples (b).

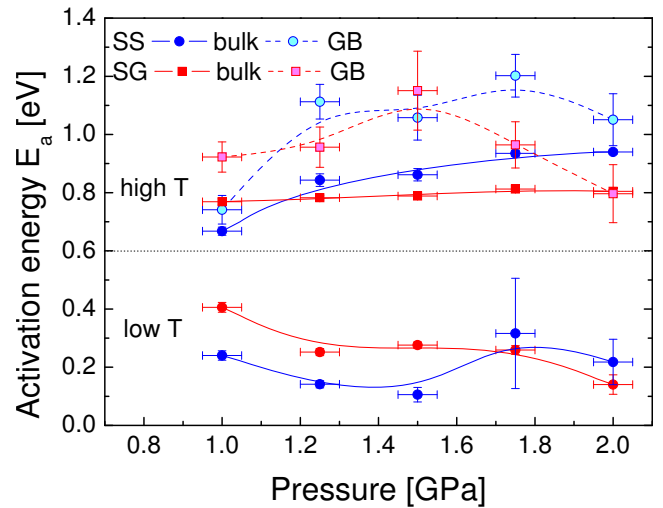


FIG. 3. (Color online) Activation energy of bulk and grain boundary conductivity for SS and SG synthesized samples at various pressures.

conductivity data in Fig. 2. At low $T < 420$ K, overall smaller E_a were found; whereas at high temperatures the increase in E_a indicated that the protons need to overcome an energy barrier to be conductive. This is in line with the previous interpretation of quasi-elastic neutron scattering (QENS) data, where in Arrhenius representation for low temperatures a flat range of proton diffusivity is found which is hardly to quantify with finite E_a because it is in the resolution limit of the experiment. This behavior was assigned to the protons trapped in a localized state.^{6,19} For higher temperatures, the E_a from QENS and impedance spectroscopy were found to be in a comparable range.^{6,7,19} The first observation is that the grain boundary E_a displayed in Fig. 3 are for the probed pressure range systematically larger than those of the bulk conductivities. For the SS derived sample, bulk E_a at 420 K $< T < 680$ K is 0.67 eV for 1 GPa and 0.94 eV for 2 GPa, and 0.77–0.80 eV for the SG derived sample, constituting a relative increase in E_a by 40% and 5%, respectively. The difference in E_a between SS and SG prepared samples can be explained by their different proton concentration. The estimated water uptake of the SG sample from thermogravimetry data collected under wet 5% H_2/Ar atmosphere from 300 to 1200 K is 0.02 mol %, ²⁰ thus we can assume it contains very few protons; whereas the proton concentration of the SS prepared sample equals 3 mol % or more.¹⁰ Furthermore, no weight loss was found from TGA in dry air in the protonated SS samples up to 723 K, which is above the maximum temperature applied during the impedance measurement.

In a recent study¹⁰ it was found that BZY10 of the nominal identical stoichiometry had E_a ranging from 0.45 to 0.80 eV, depending on how they were synthesized. They had the same crystallographic phase symmetry, but their lattice constants differed, which we interpret as a form of chemical pressure. Interestingly, the study showed a clear linear relation between the bulk E_a and lattice constant. This striking correlation implies that the crystal lattice volume constitutes a very important parameter for bulk proton conductivity.

A necessary method to compare the transport properties of all aforementioned samples with respect to the pressure is to base them on their lattice constant. Since we do not have the necessary data for the lattice parameter of BZY10 as a function of pressure, we apply literature data for $BaZrO_3$ by

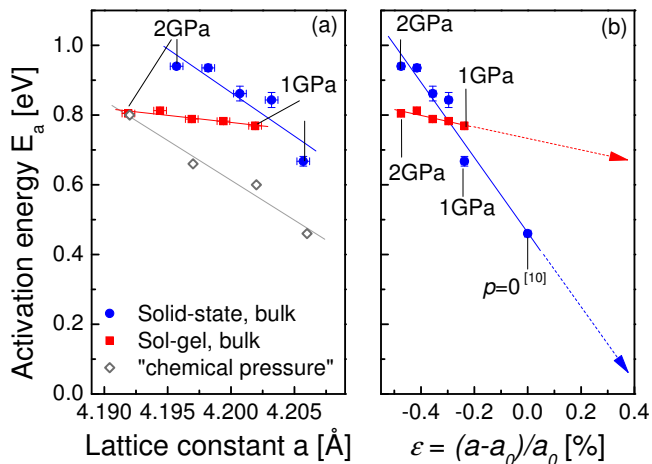


FIG. 4. (Color online) Variation in activation energy of bulk conductivity on the lattice parameter, under mechanical and “chemical” pressure (a); and on the strain parameter ϵ (b). The data point at ambient pressure was taken from Ref. 10.

Kurosaki²¹ *et al.* Combining the equilibrium lattice parameter of our SS and SG BZY10 samples from the β -phase of a much higher proton conductivity and their compressibility data²¹ for BaZrO₃, we translated pressure into lattice spacing. We assume here that the same pressure-dependent lattice parameter expansion applies for BZY10 at elevated temperature, thus it is possible to correlate the conductivity properties with the material lattice constant, as displayed in Fig. 4(a). At 1 GPa pressure, the SG sample has an E_a of 0.78 eV and a lattice parameter of 4.1925 Å. The E_a increases with increasing pressure to 0.80 eV at 2 GPa and 4.1825 Å. For the SS sample, the E_a extends over a larger range and also with a steeper slope. This representation allows us to compare also with the samples obtained by different synthesis and temperatures.¹⁰

The open symbols in Fig. 4(a) denote the E_a of the “chemical pressure” samples from ref. 10, which range from 0.45 eV for 4.206 Å to 0.8 eV at 4.192 Å with the slope. Similar to that from our SS samples. For all three classes of samples, it is evident that increasing lattice constant goes along with decreasing bulk E_a . Figure 4(a) shows now the general trend that the lowest E_a goes along with the largest lattice constant realized by the lowest pressure. Applying hydrostatic pressure has the same effect like tuning the “chemical pressure” induced by different synthesis routes and sintering temperatures.¹⁰ It is confirmed that the E_a decrease linearly with the increase in lattice constant. For the SG sample, the extent of lattice constant dependency is, however, not as large as found in ref. 10.

The changes in E_a in the grain boundary, both for SS and SG derived samples, are much more significant than those of bulk E_a revealing that grain boundary tailoring is an efficient way to enhance proton conductivity. It appears like there is a maximum value for the grain boundary E_a $p=1.5$ GPa or 1.75 GPa. At 2 GPa, E_a decreased to smaller values. This observation can be rationalized by a high pressure effect on the structure of grain boundary regions. For the SG derived samples, which have smaller crystallite size, this effect is more significant ($\sim 32\%$ decrease in E_a) than in the SS derived sample with larger crystallite size ($\sim 13\%$). Under high pressure, proton conductivity may be favored in the vicinity

of grain boundaries. However, the error bar of the grain boundary E_a is one order of magnitude higher than that from the bulk. Therefore, more temperature and pressure data are necessary for a better supported conclusion.

Our technological interest is of course not increasing the E_a by compressing, but the opposite- expanding the lattice and thus potentially lowering E_a . Considering the variation in the bulk E_a as a function of the reduced lattice parameter ratio a/a_0 or, like exercised in Fig. 4(b), on the strain parameter $\epsilon = (a - a_0)/a_0$, it is suggested that proton conductors prepared under tensile strain, i.e., $\epsilon > 0$, could have an even lower E_a and improved proton conductivity. Such situation could be realized in epitaxial strained films, for example, which also bears the possibility of having less grain boundaries that limit the proton conductivity. Stabilization of metastable proton conducting phases with tensile strain may, therefore, be a very rewarding research direction to be pursued further. It would be interesting to learn to what extent enhanced proton conductivity would be observed in expanded lattices and which additional material parameters would drive or impede this process.

Funding by E.U. MIRG Grant No. CT-2006-042095, Swiss NSF Grant No. 200021-124812, Swiss Federal Office of Energy under Project No. 100411, and Empa Director’s Fund sixth R&D Series. We are grateful to Joël Mesot (Paul Scherrer Institut) for helpful advice.

¹K. D. Kreuer, *Annu. Rev. Mater. Res.* **33**, 333 (2003).

²T. Norby, M. Widerøe, R. Glöckner, and Y. Larring, *Dalton Trans.* **19**, 3012 (2004).

³A. Braun, A. Ovalle, V. Pomjakushin, A. Cervellino, S. Erat, W. C. Stolte, and T. Graule, *Appl. Phys. Lett.* **95**, 224103 (2009).

⁴M. S. Islam, R. A. Davies, and J. D. Gale, *Chem. Commun. (Cambridge)* **2001**, 661.

⁵M. E. Björketun, P. G. Sundell, and G. Wahnström, *Phys. Rev. B* **76**, 054307 (2007).

⁶T. Matzke, U. Stimming, C. Karmonik, M. Soetratmo, R. Hempelmann, and F. Guthoff, *Solid State Ionics* **86–88**, 621 (1996).

⁷R. Hempelmann, C. Karmonik, T. Matzke, M. Cappadonia, U. Stimming, T. Springer, and M. A. Adams, *Solid State Ionics* **77**, 152 (1995).

⁸T. Scherban, W. K. Lee, and A. S. Nowick, *Solid State Ionics* **28–30**, 585 (1988).

⁹S. B. C. Duval, P. Holtappels, U. Stimming, and T. Graule, *Solid State Ionics* **179**, 1112 (2008).

¹⁰S. B. C. Duval, Dissertation, Techn. Univ. München, 2008.

¹¹A. Ashok, N. Kochetova, T. Norby, and A. Olsen, *Solid State Ionics* **179**, 1858 (2008).

¹²J. Wu, Dissertation, Caltech, 2004.

¹³B. Merinov, C. O. Dorso, W. A. Goddard, J. Wu, and S. Haile, Report No. 833847, 2003 (unpublished).

¹⁴R. Hinrichs, G. Tomandl, and J. A. H. da Jornada, *Solid State Ionics* **77**, 257 (1995).

¹⁵S. B. C. Duval, P. Holtappels, U. F. Vogt, E. Pomjakushina, K. Conder, U. Stimming, and T. Graule, *Solid State Ionics* **178**, 1437 (2007).

¹⁶A. Braun, S. Duval, P. Ried, J. Embs, F. Juranyi, T. Strässle, U. Stimming, R. Hempelmann, P. Holtappels, and T. Graule, *J. Appl. Electrochem.* **39**, 471 (2009).

¹⁷A. Azad, C. Savaniu, S. Tao, S. Duval, P. Holtappels, R. M. Ibberson, and J. T. S. Irvine, *J. Mater. Chem.* **18**, 3414 (2008).

¹⁸N. Bagdassarov, H. C. Freiheit, and A. Putnis, *Solid State Ionics* **143**, 285 (2001).

¹⁹R. Hempelmann, *Physica B* **226**, 72 (1996).

²⁰C. D. Savaniu, J. Canales-Vazquez, and J. T. S. Irvine, *J. Mater. Chem.* **15**, 598 (2005).

²¹K. Kurosaki, J. Adachi, T. Maekawa, and S. Yamanaka, *J. Alloys Compd.* **407**, 49 (2006).